

# Indentation: A simple, nondestructive method for characterizing the mechanical and transport properties of pH-sensitive hydrogels

Yuhang Hu, Jin-Oh You, Debra T. Auguste, Zhigang Suo, and Joost J. Vlassak<sup>a)</sup>  
*School of Engineering and Applied Sciences, Harvard University, Cambridge, Massachusetts 02138*

(Received 13 May 2011; accepted 30 August 2011)

We use instrumented indentation to characterize the mechanical and transport behavior of a pH-sensitive hydrogel in various aqueous buffer solutions. In the measurement, an indenter is pressed to a fixed depth into a hydrogel disk and the load on the indenter is recorded as a function of time. By analyzing the load–relaxation curve using the theory of poroelasticity, the elastic constants of the hydrogel and the diffusivity of water in the gel can be evaluated. We investigate how the pH and ionic strength of the buffer solution, the hydrogel cross-link density, and the density of functional groups on the polymer backbone affect the properties of the hydrogel. This work demonstrates the utility of indentation techniques in the characterization of pH-sensitive hydrogels.

## I. INTRODUCTION

Hydrogels are cross-linked polymer networks swollen in an aqueous solution. A number of hydrogels are stimuli-responsive; they swell in response to external stimuli, such as temperature,<sup>1</sup> electrical field,<sup>2</sup> light,<sup>3</sup> and pH.<sup>4</sup> Such responsive materials are useful in the development of microfluidic devices,<sup>5,6</sup> actuators and sensors,<sup>7,8</sup> media for cell immobilization,<sup>9</sup> and carriers for drug delivery.<sup>10–13</sup> Optimized design of these materials requires a quantitative understanding of how the mechanical and transport properties of the stimuli-responsive hydrogels change as the environment changes. A powerful and convenient characterization technique is necessary.

Among the various stimuli-responsive hydrogels, the most widely used are pH-sensitive gels because of their practical applications.<sup>5–9,13</sup> Hydrogels that are pH-sensitive contain acidic (e.g., acrylic acid) or basic (e.g., tertiary amine) functional groups that donate or accept protons in response to changes in the pH of the environment. For instance, hydrogels containing tertiary amine groups (as does the material used in this research) become protonated when the pH of the surrounding medium falls below the  $pK_a$  value of the conjugate acid of the amine groups. To maintain charge neutrality, counter ions migrate into the hydrogel together with the protons. The increased concentration of counter ions in the gel provides an osmotic driving force for the hydrogel to swell. The swelling ability of the hydrogel depends on the cross-link density of the gel, the salt concentration of the external solution, and the density of the tertiary amine groups.

The mechanical and transport properties of hydrogels have been studied by many researchers using various test methods. Widely used methods for measuring the stiffness of hydrogels include tension,<sup>14–16</sup> compression,<sup>17–19</sup> bending,<sup>20–22</sup> shearing,<sup>23</sup> cavitation,<sup>24</sup> and rheological methods,<sup>25–27</sup> as well as nano-, and macro-indentation.<sup>28–38</sup> The accessible length scale and stiffness range for each method are summarized in Table I. Poisson's ratios of hydrogels are rarely measured. When a load is suddenly applied to a hydrogel, water molecules do not have enough time to migrate into or out of the polymer network right away. Consequently, the volume of the hydrogel is conserved and the instantaneous value of Poisson's ratio is very close to 0.5.<sup>14–16</sup> Given enough time, however, water molecules diffuse into or out of the network until equilibrium is reached. The volume of the hydrogel changes and Poisson's ratio decreases to a value below 0.5.<sup>19,22,36,37,38</sup> The most widely used method for measuring the transport properties of hydrogels is based on the kinetics of the swelling process.<sup>39–43</sup> This method measures the average diffusivity of water in a hydrogel as it evolves from its dry to its swollen state. However, it has been observed experimentally that the diffusivity of hydrogels changes with water concentration,<sup>46</sup> so that this method cannot be used to measure the diffusivity of a pH-sensitive hydrogel at different pH levels.

In our recent work,<sup>36–38</sup> we proposed an indentation method for characterizing the mechanical and transport properties of hydrogels based on linear poroelasticity. The theory of poroelasticity was originally developed by Terzaghi<sup>47</sup> and Biot<sup>48</sup> to study the consolidation of soil. The indentation method proposed in our previous article<sup>35</sup> is superior to other experimental techniques in several aspects. First, most hydrogels are compliant and some of them are very slippery, so that traditional techniques such

<sup>a)</sup>Address all correspondence to this author.  
e-mail: vlassak@esag.harvard.edu  
DOI: 10.1557/jmr.2011.368

TABLE I. Existing methods for measuring mechanical and transport properties of gels.

Method	Advantage	Disadvantage
Tensile test (Refs. 14–16)	Modulus and Poisson's ratio can be measured Simple geometry for analysis	Difficult to clamp sample Sample requires uniform cross-section Only applicable to relatively stiff gels (modulus > 100 kPa) Local properties cannot be measured
Compression test (Refs. 17–19)	Modulus, Poisson's ratio, and diffusivity can be measured Simple geometry for analysis	For transport measurements, sample needs to be small to reduce measurement time Local properties cannot be measured
Beam bending (Refs. 20–22)	Modulus, Poisson's ratio, and diffusivity can be measured Boundary value problem is simple	Only applicable to stiff gels (modulus > MPa) Local properties cannot be measured
Shear (Ref. 23)	Shear modulus can be measured	Not possible to measure transport properties
Cavitation (Ref. 24)	Modulus can be measured Setup and handling are simple Local properties can be measured	Only instantaneous modulus is measured Diffusivity cannot be measured
Microbead rheology (Refs. 25–27)	Modulus can be measured Viscoelasticity can be characterized	Only used for uncross-linked polymer solutions or lightly cross-linked gels (modulus < 100 Pa) Data interpretation is difficult
Swelling kinetics (Refs. 39–43)	Diffusivity can be measured	For small samples, tracing of fluorescent particles may be required Local properties cannot be measured
Transport through membrane (Refs. 44,45)	Diffusivity can be measured	Modulus cannot be measured Very difficult measurement Local properties cannot be measured Modulus cannot be measured Specific transport model is required
Nanoscale indentation (Refs. 28–31)	Modulus can be measured Viscoelasticity can be characterized Local properties can be measured	Equipment is expensive Contact point is hard to detect
Macroscale indentation (Refs. 32–38)	Modulus, Poisson's ratio, and diffusivity can be measured Simple experimental setup Minimum specimen preparation	Large sample is required (>5mm)

as tensile, bending, and torsion testing can only with difficulty be applied to gels. Indentation experiments, in contrast, do not require much sample handling and are readily performed on a hydrogel. Second, both the mechanical and transport properties of a hydrogel can be obtained through a single indentation measurement. These properties can be measured at different hydration states, corresponding to specific salt concentrations and/or pH levels of the external medium. In this article, we demonstrate the indentation load relaxation technique by measuring the mechanical and transport properties of various hydrogel formulations (cross-link density and composition) under a range of environmental conditions (pH and salt concentration of the external solution).

## II. THE INDENTATION LOAD RELAXATION METHOD

The geometry of the indentation method is shown in Fig. 1. An indenter is pressed to a depth  $h$  into a gel submerged in a solvent, and the force on the indenter is recorded as a function of time. As the force on the indenter relaxes, the contact area between the indenter and gel

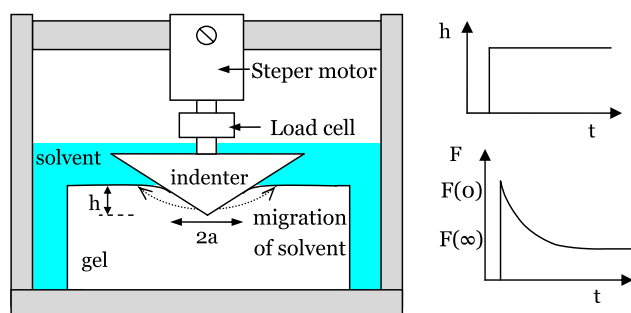


FIG. 1. A disk of a gel is submerged in a solvent throughout the experiment. Prior to indentation, the gel imbibes the solvent and swells to a state of equilibrium. An indenter is then rapidly pressed into the gel and is subsequently held at a fixed depth  $h$ . The indenter causes the solvent to migrate in the gel, so that the force  $F$  on the indenter decreases as a function of time, until the gel reaches a new state of equilibrium.

remains unchanged.<sup>32,36</sup> In the short-time limit, the concentration of solvent molecules in the gel is constant, i.e., the gel behaves like an incompressible elastic material with a shear modulus  $G$ . For a conical indenter pressed into an incompressible elastic material, the force on the indenter is given by<sup>49</sup>

$$F(0) = 4Gah \quad (1)$$

where  $F(0)$  is the instantaneous force on the indenter. The radius of contact  $a$  relates to the depth of indentation  $h$  as

$$a = \frac{2}{\pi} h \tan \theta \quad (2)$$

where  $\theta$  is half the included angle of the conical indenter.

In the long-time limit, the gel attains a new state of equilibrium and the solvent in the gel equilibrates with the external solvent. The gel now behaves like a compressible elastic material with shear modulus  $G$  and Poisson's ratio  $\nu$ . The force in the long-time limit,  $F(\infty)$ , is related to the instantaneous force,  $F(0)$ , by<sup>36</sup>

$$F(0)/F(\infty) = 2(1 - \nu) \quad (3)$$

For the gel to evolve from the short-time to the long-time limit, the solvent in the gel under the indenter must migrate. The relevant length scale is the radius of the contact area between the indenter and the gel. The time required for diffusion to occur over this distance scales with  $a^2 / D$  and indeed the force on the indenter,  $F(t)$ , obeys the following equation<sup>36</sup>

$$\frac{F(t) - F(\infty)}{F(0) - F(\infty)} = g(\tau) \quad (4)$$

where  $\tau = Dt / a^2$  is a nondimensional time. The dimensionless ratio on the left-hand side of Eq. (4) is a measure of how far the gel is from equilibrium. The function  $g(\tau)$  must be determined by solving the poroelastic boundary value problem. Our previous work indicates that, for a given type of indenter,  $g$  is a function of the single variable  $\tau$ , as long as the radius of contact is much smaller than the size of the disk of the gel. The poroelastic boundary value problem was solved for indenters of various shapes using the finite element method<sup>36</sup> and the function  $g(\tau)$  for a conical indenter is given by the following expression

$$g(\tau) = 0.493 \exp(-0.822\sqrt{\tau}) + 0.507 \exp(-1.348\tau) \quad (5)$$

### III. EXPERIMENTS

#### A. Synthesis

Hydrogels were synthesized using dimethylaminoethylmethacrylate (DMAEMA) and acrylamide (AAm) monomers, N,N'-methylenebisacrylamide (MBAAm) as a cross-linker, and ammonium persulfate (APS) as an initiator. AAm, MBAAm, and APS were purchased from

Sigma-Aldrich Inc. (Atlanta, GA). DMAEMA was acquired from Fisher Scientific Company (Boston, MA). The chemical structures of the agents are shown in Fig. 2. AAm is a neutral monomer, while DMAEMA is a hydrophobic monomer with cationic groups. Buffer solutions were prepared by mixing sodium phosphate monobasic and sodium phosphate dibasic heptahydrate obtained from Sigma-Aldrich Inc. in the appropriate ratios as described by reference 50.

Four sets of poly (DMAEMA-co-AAm) hydrogel samples<sup>50</sup> were synthesized as listed in Table II. The following formulation was used to make the samples in the first set. First, a monomer solution was prepared by mixing 6.67 mL DMAEMA and 6.67 g AAm with 10 mL deionized water. The cross-linker and initiator solutions were prepared by dissolving 166.7 mg MBAAm in 6.67 mL deionized water and 330 mg APS in 6.67 mL deionized water, respectively. The MBAAm and APS solutions were mixed and then poured into the monomer solution. The mixture was gently mixed for 40 s and then poured into a glass petri dish with an inner radius of 52 mm. After allowing the hydrogel to polymerize for 2 h, the gel was removed from the petri dish and individual gel samples were submerged into 10 mM sodium phosphate buffer solutions of various pH as listed in Table II. Samples were submerged for a period of at least 2 weeks to allow them to swell. After 2 weeks, no more changes in the dimensions of the samples were observed and the samples were assumed to be in equilibrium with the buffer solutions. Indeed, the time needed for water to be transported throughout a sample with a thickness  $H$  of approximately  $10^{-2}$  m and a minimum diffusivity  $D$  of  $10^{-10}$  m<sup>2</sup>/s is on the order of  $H^2/D \sim 10^6$  s, i.e., 2 weeks are sufficient time for the samples to equilibrate. These gels are used as baseline in the experiments and are denoted as "REF." In addition, three more sets of gels were fabricated following the same procedure but with different amounts of chemicals and/or buffer solutions as indicated in Table II: one set of gels was fabricated and submerged in a 100 mM buffer solution—this set of gels is denoted as "Salt-Hi." Another set was fabricated

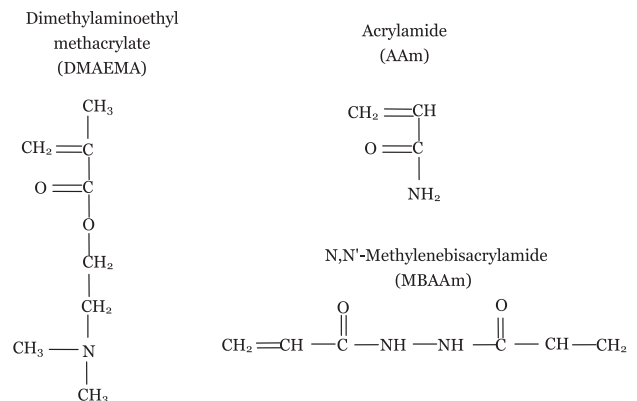


FIG. 2. Chemical structures of dimethylaminoethylmethacrylate and acrylamide monomers and N,N'-methylenebisacrylamide cross-linker.

TABLE II. Compositions of the factors that influence the mechanical and transport properties of the poly(DMAEMA-co-AAm) hydrogels.

Code	Salt concentration (mM)	Amount of cross-linker (mg)	Amount of DMAEMA (mL)	Amount of AAm polymer (g)
REF	10	166.7	6.67	6.67
Salt-Hi	100	166.7	6.67	6.67
XL-Lo	10	100	6.67	6.67
Salt-Hi-DMAEMA/AAm-Hi	100	166.7	9	4.5

using 100 mg of cross-linker and is denoted as “XL-Lo.” A last set of gels had a larger ratio of DMAEMA to AAm and was submerged in a 100 mM buffer solution. This set of gels is referred to as “Salt-Hi-DMAEMA/AAm-Hi.”

The weights of the swollen samples,  $w_{\text{gel}}$ , were measured after superficially drying the samples with a paper towel, and the swelling ratio  $\lambda$  was calculated from

$$\lambda = \left( \frac{(w_{\text{gel}} - w_{\text{dry}})/\rho_w}{w_{\text{dry}}/\rho_d} + 1 \right)^{1/3}, \quad (6)$$

where  $\rho_w$  and  $\rho_d$  are the densities of water and the dry polymer network, respectively. The weights,  $w_{\text{dry}}$ , and densities of the dry hydrogels were calculated from the weights of the individual components of the polymer networks and their respective densities.

## B. Indentation measurements

The indentation load relaxation measurements were performed using a stainless steel conical indenter with a half included angle of  $\theta = 70^\circ$ . The indenter was pressed into the samples using a custom-built load frame with a force resolution of 0.5 mN and a displacement resolution of 1  $\mu\text{m}$ . The indenter approached the surface of the gels at a constant speed of 2  $\mu\text{m/s}$  until the slope of the recorded force–displacement curve became positive. The position of the surface was then determined by back extrapolation. The error in the position of the surface using this methodology was less than 5  $\mu\text{m}$  for all measurements. Once the surface was found, the indenter was pressed into the samples at a constant speed of 300  $\mu\text{m/s}$ , the maximum speed allowed by the load frame. During the experiments, the force on the indenter was recorded as a function of time. The time used to press the indenter into the gel ( $\sim 2$  s) was much shorter than the relaxation time recorded experimentally (hours), so that any poroelastic relaxation during the initial loading segment was entirely negligible. Indentations were performed to three different depths, 400, 600, and 800  $\mu\text{m}$ . For each depth, three load–relaxation measurements were carried out. In total, nine relaxation curves were recorded for each sample. The length of time for the load to fully relax was determined during the experiments by visual inspection of the relaxation curves. To ascertain the load was fully relaxed, data was recorded for an additional period of time equal to two times the

relaxation time. All measurements were performed with the samples submerged in the appropriate buffer solution. The effects of the ionic strength of the buffer solutions, the cross-link density, and the amine group density on the properties of the hydrogel were evaluated using the samples in different sets. Indentations on these samples were performed using the same experimental protocol as for the samples in the baseline set.

## IV. RESULTS AND DISCUSSION

### A. Swelling ratio

Figure 3 shows as a function of pH the change in sample mass between the dry and the swollen state. Compared with REF gels, the Salt-Hi gels swelled in buffer solutions of higher salt concentrations. Evidently the pH sensitivity of the gel decreases with increasing salt concentration. When the gel is put in an aqueous solution with a pH below the  $\text{p}K_a$  of the amines on the polymer network, the amine groups are protonated. To maintain charge neutrality, counter ions need to migrate into the gel along with the protons. If the salt concentration of the buffer solution is high, the change in the concentration of counter ions inside the gel induces only a small change in the osmotic pressure and consequently only a small increase in swelling.

The effect of cross-link density on swelling is illustrated by comparing the results for REF gels and XL-Lo gels. Figure 6 shows that in the same buffer solutions, XL-Lo gels swell significantly more than REF gels. In equilibrium, the degree of swelling is determined by the balance between the osmotic driving force for water to enter the gel network and the elastic energy stored in the network. As the cross-link density increases, the network becomes stiffer and the amount of swelling is reduced.

The influence of the ratio between the two monomers (DMAEMA and AAm) is illustrated by comparing the results for Salt-Hi gels and Salt-Hi-DMAEMA/AAm-Hi gels. For Salt-Hi gels, the ratio of DMAEMA to AAm is 1:1 in weight, while for Salt-Hi-DMAEMA/AAm-Hi gels, the ratio is 2:1, i.e., the Salt-Hi-DMAEMA/AAm-Hi gels contain more tertiary amine groups. Consequently, when these amine groups are protonated, the Salt-Hi-DMAEMA/AAm-Hi gels require a greater concentration of counter ions than Salt-Hi gels. This in turn creates a greater osmotic pressure driving water molecules into the gel and the degree of swelling increases. A similar trend was observed

by You and Auguste<sup>13</sup> in their study of DMAEMA/HEMA (2-hydroxyethyl methacrylate) nanoparticles to regulate gene transfer.

### B. Mechanical properties

Figure 4 shows the force–relaxation curves for five different pH levels obtained for the REF gels. Three curves are shown for each of three indentation depths. Figure 5 depicts the same data with force normalized as  $F/ah$  and time as  $t/a^2$ . It is evident from the figure that the nine relaxation curves obtained for each pH level collapse into a single curve. This behavior is consistent with poroelastic behavior of the hydrogel. That the curves from samples swollen in different buffer solutions do not collapse is an

indication that the mechanical and transport properties of the gel change with pH. The shear modulus and Poisson’s ratio were calculated using Eqs. (1) and (3), while the diffusivity was extracted by fitting the theoretical curve, Eq. (5), to the experimental data. When the results are properly scaled, all 45 load–relaxation curves collapse into a single master curve as illustrated in Fig. 6. The dashed line in Fig. 6 represents the theoretical curve given by Eq. (5). The experimental results for the gels in the other three sets were evaluated using the same analysis. All material parameters obtained for each set of gels, including shear modulus, Poisson’s ratio, and diffusivity are summarized in Table III.

Figure 7 shows the shear moduli for the four sample sets as a function of buffer solution pH. As each gel swells, its shear modulus decreases because the number of chains per unit volume is reduced. Decreasing the cross-link density, increasing the ratio of DMAEMA to AAm, or decreasing the salt concentration increases the swelling ratio of the gels and thus lowers their shear modulus. A similar trend was reported for other pH-sensitive gels.<sup>14</sup> The thermodynamic properties of gels have been investigated extensively by Flory.<sup>51</sup> According to Flory–Huggins’ theory, the shear modulus of a neutral gel can be related to its swelling ratio by<sup>37</sup>

$$Nk_B T = \lambda G_{\text{gel}} \quad (7)$$

where  $k_B T$  is temperature in units of energy and  $N$  is the number of polymer chains in the gel divided by the volume of the dry polymer, a measure for the cross-link density of the gel. Thus, according to the Flory–Huggins’ model,

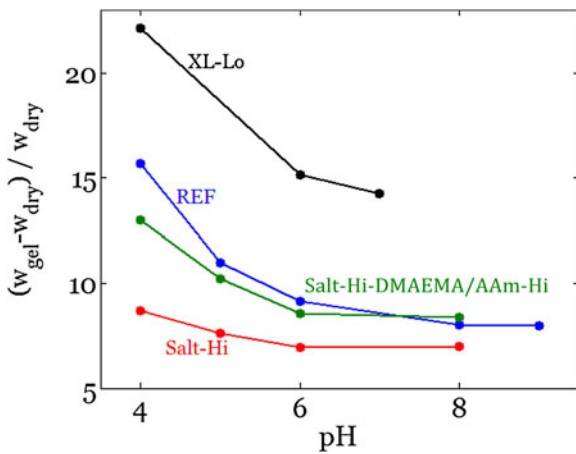


FIG. 3. Gravimetric swelling ratios for the four sets of gels as a function of pH.

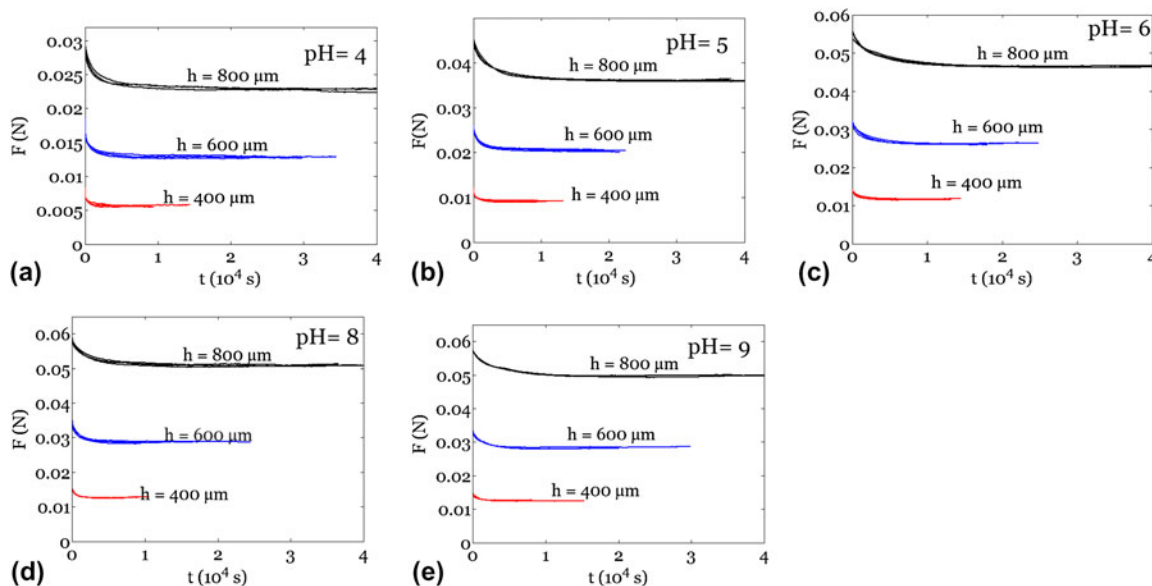


FIG. 4. Experimentally measured force–relaxation curves for the REF gel. The pH values of the buffer solutions are (a) pH = 4, (b) pH = 5, (c) pH = 6, (d) pH = 8, and (e) pH = 9.

$\lambda G_{\text{gel}}$  should be constant. Figure 8 shows the experimental values of  $\lambda G_{\text{gel}}$  for each set of samples as a function of pH. It can be observed that  $\lambda G_{\text{gel}}$  is constant at high pH levels but decreases below pH 6. Evidently, Eq. (7) breaks down

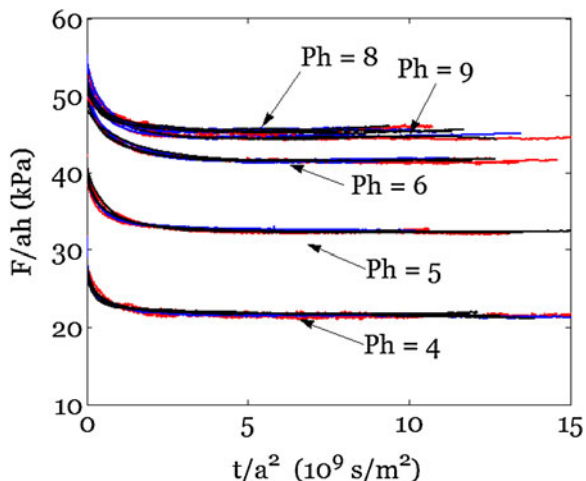


FIG. 5. Experimental stress–relaxation curves for the REF gel. The force is normalized as  $F / ah$ , and the time is normalized as  $t / a^2$ .

for poly-(DMAEMA-co-AAm) in this pH range. One likely reason is the presence of electric charges associated with the protonated amine groups on the polymer chains. The precise mechanism of how these charges affect the stiffness of the gel is at present unknown, and a good mechanical model for polyelectrolyte gels such as the one studied here remains to be developed.

Poisson’s ratio describes the architecture of a network via the lateral-to-axial strain ratio. Few studies have been performed on measuring the Poisson’s ratio of hydrogels. Determining Poisson’s ratio of a gel quantitatively is more complicated than for solid materials because it involves the flow of solvents. When an external load is suddenly applied to a gel, there is initially not enough time for the solvent to migrate out of or into the gel. Consequently, the gel is incompressible and Poisson’s ratio approaches 0.5. In most previous studies, Poisson’s ratio was measured in the near instantaneous state using the tensile test.<sup>14–16</sup> In this study, however, Poisson’s ratio is defined as the ratio of lateral to vertical strain when the gel is in its equilibrium state. Since a certain amount of solvent has been squeezed out of or absorbed into the gel to attain equilibrium, the equilibrium value of Poisson’s ratio is smaller than 0.5.

TABLE III. Measured swelling ratio, shear modulus, Poisson’s ratio, and diffusivity of four sets of gels in various pH solutions.

	REF gels				
	pH = 4	pH = 5	pH = 6	pH = 8	pH = 9
$(w_{\text{gel}} - w_{\text{dry}}) / w_{\text{dry}}$	15.69	10.98	9.16	8.03	7.99
Shear modulus, $G$ (kPa)	$7.06 \pm 0.68$	$10.28 \pm 0.94$	$12.28 \pm 0.72$	$13.15 \pm 1.02$	$12.61 \pm 1.18$
Poisson’s ratio, $\nu$	$0.31 \pm 0.02$	$0.36 \pm 0.01$	$0.40 \pm 0.01$	$0.41 \pm 0.01$	$0.42 \pm 0.01$
Diffusivity, $D$ ( $10^{-10}$ m <sup>2</sup> /s)	$13.1 \pm 2.1$	$11.3 \pm 3.9$	$7.0 \pm 2.3$	$7.9 \pm 2.2$	$6.2 \pm 3.4$
Permeability, $k$ ( $10^{-17}$ m <sup>2</sup> )	$4.54 \pm 0.36$	$2.14 \pm 0.37$	$0.85 \pm 0.14$	$0.82 \pm 0.11$	$0.6 \pm 0.17$
	Salt-Hi gels				
	pH = 4	pH = 5	pH = 6	pH = 8	
$(w_{\text{gel}} - w_{\text{dry}}) / w_{\text{dry}}$	8.69	7.62	6.96	7.01	
Shear modulus, $G$ (kPa)	$12.06 \pm 0.33$	$12.80 \pm 0.38$	$14.70 \pm 0.22$	$14.54 \pm 0.23$	
Poisson’s ratio, $\nu$	$0.37 \pm 0.02$	$0.38 \pm 0.02$	$0.41 \pm 0.01$	$0.425 \pm 0.01$	
Diffusivity, $D$ ( $10^{-10}$ m <sup>2</sup> /s)	$9.6 \pm 3.1$	$8.1 \pm 2.0$	$7.4 \pm 2.6$	$6.3 \pm 3.3$	
Permeability, $k$ ( $10^{-17}$ m <sup>2</sup> )	$1.46 \pm 0.24$	$1.09 \pm 0.13$	$0.68 \pm 0.12$	$0.47 \pm 0.12$	
	XL-Lo gels				
	pH = 4	pH = 6	pH = 7		
$(w_{\text{gel}} - w_{\text{dry}}) / w_{\text{dry}}$	22.12	15.16	14.24		
Shear modulus, $G$ (kPa)	$3.89 \pm 0.39$	$6.12 \pm 0.31$	$6.35 \pm 0.35$		
Poisson’s ratio, $\nu$	$0.39 \pm 0.02$	$0.42 \pm 0.01$	$0.43 \pm 0.01$		
Diffusivity, $D$ ( $10^{-10}$ m <sup>2</sup> /s)	$9.8 \pm 2.7$	$8.2 \pm 2.3$	$8.1 \pm 3.3$		
Permeability, $k$ ( $10^{-17}$ m <sup>2</sup> )	$4.04 \pm 0.56$	$1.64 \pm 0.23$	$1.39 \pm 0.28$		
	Salt-Hi-DMAEMA/AAm-Hi gels				
	pH = 4	pH = 5	pH = 6	pH = 8	
$(w_{\text{gel}} - w_{\text{dry}}) / w_{\text{dry}}$	13.01	10.22	8.56	8.36	
Shear modulus, $G$ (kPa)	$2.25 \pm 0.21$	$4.22 \pm 0.15$	$4.86 \pm 0.18$	$4.74 \pm 0.09$	
Poisson’s ratio, $\nu$	$0.32 \pm 0.02$	$0.39 \pm 0.01$	$0.40 \pm 0.01$	$0.39 \pm 0.01$	
Diffusivity, $D$ ( $10^{-10}$ m <sup>2</sup> /s)	$18 \pm 3.4$	$15 \pm 3.1$	$7.2 \pm 2.7$	$6.8 \pm 2.3$	
Permeability, $k$ ( $10^{-17}$ m <sup>2</sup> )	$18.84 \pm 1.78$	$5.7 \pm 0.59$	$2.2 \pm 0.41$	$2.3 \pm 0.39$	

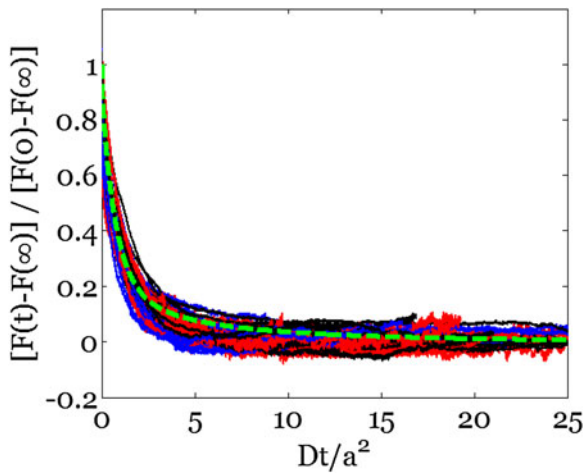


FIG. 6. Experimental stress–relaxation curves for the REF gel. The force is normalized as  $[F(t) - F(\infty)] / [F(0) - F(\infty)]$ , and the time is normalized as  $Dt / a^2$ . For the experimental data to fit the function  $g(\tau)$ , each buffer solution needs a distinct value of  $D$ , as listed in Table III.

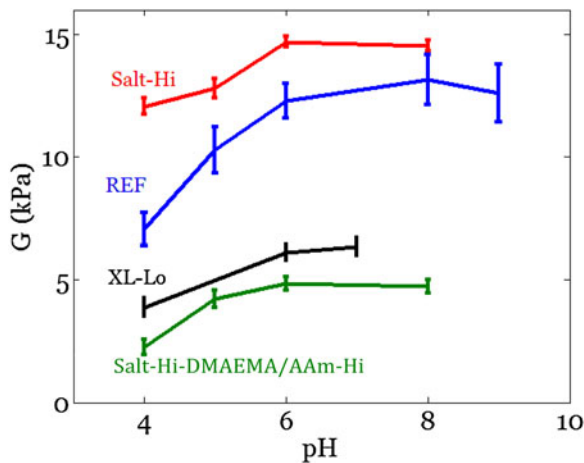


FIG. 7. Experimental shear moduli for the four sets of gels plotted as a function of pH.

Figure 9 shows Poisson’s ratio as a function of pH. It is observed that Poisson’s ratio decreases with decreasing pH, i.e., with increasing swelling ratio. To appreciate the physical significance of Poisson’s ratio of a poroelastic material, consider a hypothetical experiment involving compression of a cylindrical gel of diameter  $A$  and thickness  $L$  in the axial direction. The gel cylinder is submerged in a solvent and a fixed strain  $\varepsilon$  is imposed. Initially solvent molecules do not have enough time to migrate into or out of the network, and the gel cylinder acts as an incompressible material with diameter  $A(1 + \varepsilon / 2)$  and thickness  $L(1 - \varepsilon)$ . The compression increases the chemical potential of the solvent within the gel above the value of the external solvent. This inequality of chemical potential drives the solvent molecules to migrate out of the gel. In the equilibrium state, the diameter of the gel cylinder

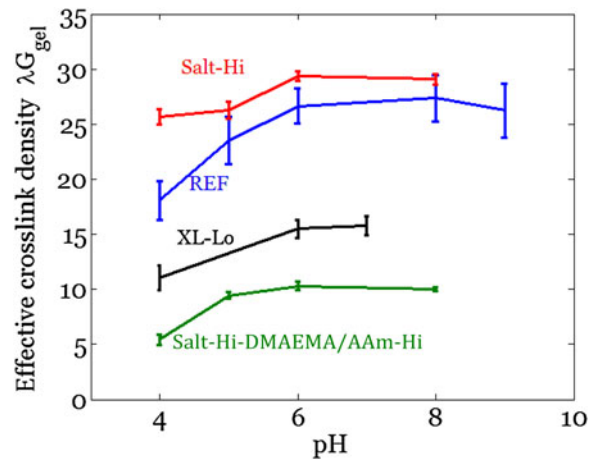


FIG. 8. Experimental values of the effective cross-link density  $\lambda G_{\text{gel}}$  (Eq. 7) for the four sets of gels plotted as a function of pH.

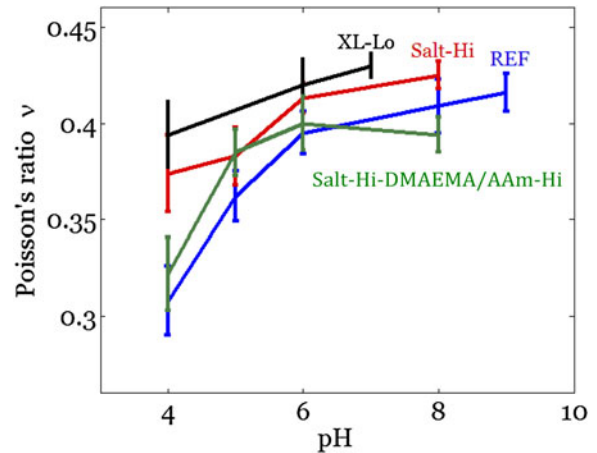


FIG. 9. Experimental Poisson’s ratios for the four sets of gels plotted as a function of pH.

decreases to  $A(1 + \nu\varepsilon)$ . Thus, a smaller value of  $\nu$  implies that more solvent migrates out of the gel. The experimental results (Fig. 9) show that it is easier to squeeze the solvent out of the gel as the degree of swelling increases.

### C. Water diffusivity

The time-dependent behavior of hydrogels is limited by the diffusion of water molecules. It has been observed that the diffusivity of water in hydrogels depends on the solvent concentration of water.<sup>46</sup> Currently, the most widely used method for measuring the diffusivity of hydrogels is based on swelling kinetics.<sup>39–43</sup> The diffusivity measured using this method is an average value for the gel as it changes from the dry state to the swollen state. In this study, the gel samples were first submerged and equilibrated in an aqueous solution. The indentation measurements were then performed on these samples. Consequently, the water diffusivity measured in the indentation experiments is the

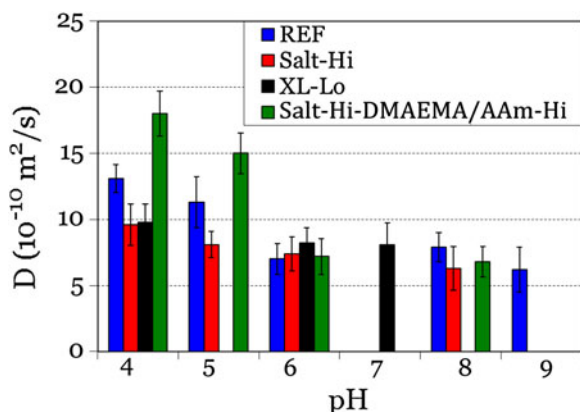


FIG. 10. Experimental water diffusivities for the four sets of gels plotted as a function of pH.

value at that particular water concentration. Figure 10 shows the water diffusivity in each sample as a function of pH. The diffusivity is constant at large pH values but increases when the pH drops below 6. This is consistent with water molecules migrating faster in a network of large mesh size than in a network of small mesh size. This trend has also been observed in other gels.<sup>53</sup>

Based on Darcy's law, the diffusivity is related to the permeability of the gel,  $k$ , by

$$D = \frac{2(1 - \nu)Gk}{(1 - 2\nu)\eta}, \quad (8)$$

where  $\eta$  is the viscosity of the solvent. The permeability of each sample was calculated using a water viscosity of  $8.9 \times 10^{-4} \text{ Pa}\cdot\text{s}$  and is listed in Table III.

## V. CONCLUSION

In this article, we have used instrumented indentation to characterize the mechanical and transport properties of a series of pH-sensitive hydrogels. The influence of solution pH, solution ionic strength, cross-link density of the polymer network, and the density of functional groups on the mechanical and transport properties of the hydrogel has been evaluated. In general, the shear modulus and Poisson's ratio of the hydrogel decrease as it swells, while water diffusivity increases. Unlike neutral gels, the stiffness of the pH-sensitive gel at low pH values is not well described by the Flory–Huggins' model. We attribute this to the presence of electric charges associated with the protonated amine groups on the polymer chains, although the detailed mechanism is not clear at present. The indentation load relaxation measurement was proved a convenient and effective method for hydrogels in various environments.

## ACKNOWLEDGMENTS

This work is supported by the National Science Foundation (NSF) (CMMI-0800161), Multidisciplinary

University Research Initiative (MURI) (W911NF-09-1-0476), and the Materials Research Science and Engineering Center at Harvard University (DMR-0820484). The authors are grateful to Li Han for help with the experimental setup. This material is based upon work supported by the Space and Naval Warfare Systems Command (SPAWAR) Award Number N66001-09-1-2110. Any opinions, findings, and conclusions or recommendations expressed in this publication are those of the authors and do not necessarily reflect the views of SPAWAR.

## REFERENCES

1. T. Tanaka: Collapse of gels and the critical endpoint. *Phys. Rev. Lett.* **40**, 820 (1978).
2. T. Tanaka, I. Nishio, S-T. Sun, and S. Ueno-Nishio: Collapse of gels in an electric field. *Science* **218**, 467 (1982).
3. A. Suzuki and T. Tanaka: Phase transition in polymer gels induced by visible light. *Nature* **346**, 345 (1990).
4. T. Tanaka and D. Fillmore, S-T. Sun, I. Nishio, G. Swislow, and A. Shah: Phase transitions in ionic gels. *Phys. Rev. Lett.* **45**, 1636 (1980).
5. L. Dong, A.K. Agarwal, D.J. Beebe, and H. Jiang: Adaptive liquid microlenses activated by stimuli-responsive hydrogels. *Nature* **442**, 551 (2006).
6. D. J. Beebe, J. S. Moore, J. M. Bauer, Q. Yu, R. H. Liu, C. Devadoss, and B-H. Jo: Functional hydrogel structures for autonomous flow control inside microfluidic channels. *Nature* **404**, 588 (2000).
7. A. Richter, G. Paschew, S. Klatt, J. Lienig, K-F. Arndt, and H-J.P. Adler: Review on hydrogel-based pH sensors and microsensors. *Sensors* **8**, 561 (2008).
8. G. Gerlach, M. Guenther, J. Sorber, G. Subchaneck, K-F. Arndt, and A. Richter: Chemical and pH sensors based on the swelling behavior of hydrogels. *Sens. Actuat. B* **111-112**, 555 (2005).
9. A.C. Jen, M.C. Wake, and A.G. Mikos: Review: Hydrogels for cell immobilization. *Biotechnol. Bioeng.* **50**, 357 (1996).
10. B. Jeong, Y.H. Bae, D.S. Lee, and S.W. Kim: Biodegradable block copolymers as injectable drug delivery systems. *Nature* **388**, 860 (1997).
11. Y. Qiu and K. Park: Environment-sensitive hydrogels for drug delivery. *Adv. Drug Delivery Rev.* **53**, 321 (2001).
12. T.R. Hoare and D.S. Kohane: Hydrogels in drug delivery: Progress and challenges. *Polymer* **49**, 1993 (2008).
13. J. You and D.T. Auguste: Nanocarrier cross-linking density and pH sensitivity regulate intracellular gene transfer. *Nano Lett.* **9**, 4467 (2009).
14. B.D. Johnson, D.J. Beebe, and W.C. Crone: Effects of swelling on the mechanical properties of pH-sensitive hydrogel for use in microfluidic devices. *Mater. Sci. Eng., C* **24**, 575 (2004).
15. S.P. Marra, K.T. Ramesh, and A.S. Douglas: Mechanical characterization of active poly(vinyl alcohol)-poly(acrylic acid) gel. *Mater. Sci. Eng., C* **14**, 25 (2001).
16. K. Urayama, T. Takigawa, and T. Masuda: Poisson's ratio of poly(vinyl alcohol) gels. *Macromolecules* **26**, 3092 (1993).
17. E.C. Muniz and G. Geuskens: Compressive elastic modulus of polyacrylamide hydrogels and semi-IPNs with poly(N-isopropylacrylamide). *Macromolecules* **34**, 4480 (2001).
18. X. Zhao, N. Huebsch, D.J. Mooney, and Z. Suo: Stress-relaxation behavior in gels with ionic and covalent crosslinks. *J. Appl. Phys.* **107**, 063509 (2010).



19. S. Cai, Y. Hu, X. Zhao, and Z. Suo: Poroelasticity of a covalently crosslinked alginate hydrogel under compression. *J. Appl. Phys.* **108**, 113514 (2010).
20. X. Zhang, Z. Hu, and Y. Li: Bending of bi-gels. *J. Chem. Phys.* **105**, 3794 (1996).
21. G.W. Scherer: Measuring permeability of rigid materials by a beam-bending method: I. Theory. *J. Am. Ceram. Soc.* **83**, 2231 (2000).
22. W. Vichit-Vadakan and G.W. Scherer: Measuring permeability of rigid materials by a beam-bending method: II. Porous glass. *J. Am. Ceram. Soc.* **83**, 2240 (2000).
23. J.A. Stammen, S. Williams, D.N. Ku, and R.E. Gulberg: Mechanical properties of a novel PVA hydrogel in shear and unconfined compression. *Biomaterials* **22**, 799 (2001).
24. J.A. Zimmerlin, N. Sanabria-Delong, G.N. Tew, and A.J. Crosby: Cavitation rheology for soft materials. *Soft Matter* **3**, 763 (2007).
25. T.G. Mason and D.A. Weitz: Optical measurements of frequency-dependent linear viscoelastic moduli of complex fluids. *Phys. Rev. Lett.* **74**, 1250 (1995).
26. F.C. MacKintosh and C.F. Schmidt: Microrheology. *Curr. Opin. Colloid Interface Sci.* **4**, 300 (1999).
27. A. Mukhopadhyay and S. Granick: Micro- and nanorheology. *Curr. Opin. Colloid Interface Sci.* **6**, 423 (2001).
28. D.M. Ebenstein and L.A. Pruitt: Nanoindentation of biological materials. *Nano Today* **1**, 26 (2006).
29. G. Constantinides, Z.I. Kalcioğlu, M. McFarland, J.F. Smith, and K.J. Van Vliet: Probing mechanical properties of fully hydrated gels and biological tissues. *J. Biomech.* **41**, 3285 (2008).
30. J.D. Kaufman, G.J. Miller, E.F. Morgan, and C.M. Klapperich: Time-dependent mechanical characterization of poly(2-hydroxyethyl methacrylate) hydrogels using nanoindentation and unconfined compression. *J. Mater. Res.* **23**, 1472 (2008).
31. M. Galli, K.S.C. Comley, T.A.V. Shean, and M.L. Oyen: Viscoelastic and poroelastic mechanical characterization of hydrated gels. *J. Mater. Res.* **24**, 973 (2009).
32. C.Y. Hui, Y.Y. Lin, F.C. Chuang, K.R. Shull, and W.C. Ling: A contact mechanics method for characterizing the elastic properties and permeability of gels. *J. Polym. Sci., part B: Polym. Phys.* **43**, 359 (2006).
33. Y.Y. Lin and B.W. Hu: Load relaxation of a flat rigid circular indenter on a gel half space. *J. Non-Cryst. Solids* **352**, 4034 (2006).
34. W.C. Lin, K.R. Shull, C.Y. Hui, and Y.Y. Lin: Contact measurement of internal fluid flow within poly(n-isopropylacrylamide) gels. *J. Chem. Phys.* **127**, 094906 (2007).
35. M. Galli and M.L. Oyen: Fast identification of poroelastic parameters from indentation tests. *Comput. Model. Eng. Sci.* **48**, 241 (2009).
36. Y. Hu, X. Zhao, J.J. Vlassak, and Z. Suo: Using indentation to characterize the poroelasticity of gels. *Appl. Phys. Lett.* **96**, 121904 (2010).
37. Y. Hu, X. Chen, G.M. Whitesides, J.J. Vlassak, and Z. Suo: Indentation of polydimethylsiloxane submerged in organic solvents. *J. Mater. Res.* **26**(6), 785 (2011).
38. Y. Hu, E.P. Chan, J.J. Vlassak, and Z. Suo: Poroelastic relaxation indentation of thin layers of gels. *J. Appl. Phys.* **110**, 086103 (2011).
39. Y. Li and T. Tanaka: Kinetics of swelling and shrinking of gels. *J. Chem. Phys.* **92**, 1365 (1990).
40. M. Doi: Gel dynamics. *J. Phys. Soc. Jpn.* **78**, 052001 (2009).
41. S.K. De, N.R. Aluru, B. Johnson, W.C. Crone, D.J. Beebe, and J. Moore: Equilibrium swelling and kinetics of pH-responsive hydrogels: Models, experiments, and simulations. *J. Microelectromech. Syst.* **11**, 544 (2002).
42. T. Traitel, Y. Cohen, and J. Kost: Characterization of glucose-sensitive insulin release systems in simulated in vivo conditions. *Biomaterials* **21**, 1679 (2000).
43. L. Brannon-Peppas and K.A. Peppas: Time-dependent response of ionic polymer networks to pH and ionic strength changes. *Int. J. Pharm.* **70**, 53 (1991).
44. C.L. Bell and N.A. Peppas: Water, solute and protein diffusion in physiologically responsive hydrogels of poly(methacrylic acid-g-ethylene glycol). *Biomaterials* **17**, 1203 (1996).
45. G.L. Pishko, S.J. Lee, P. Wanakule, and M. Sartinorant: Hydraulic permeability of a hydrogel-based contact lens membrane for low flow rates. *J. Appl. Polym. Sci.* **104**, 3730 (2007).
46. E.J. Lightfoot: Kinetic diffusion in polymer gels. *Physica A* **169**, 191 (1990).
47. K. Terzaghi: Die berechnung der durchlässigkeitsziffer des tones aus dem verlauf der hydrodynamischen spannungsercheinungen. *Sitzungsber. Akad. Wiss. Wien Math. -Naturwiss. Kl., Abt. IIa.* **132**, 125 (1923).
48. M.A. Biot: General theory of three-dimensional consolidation. *J. Appl. Phys.* **12**, 155 (1941).
49. I.N. Sneddon: The relation between load and penetration in the axisymmetric Boussinesq problem for a punch of arbitrary profile. *Int. J. Eng. Sci.* **3**, 47 (1965).
50. B. Yıldız, B. Işık, M. Kış, and Ö. Birgül: pH-sensitive dimethylaminoethyl methacrylate (DMAEMA)/acrylamide (AAm) hydrogels: Synthesis and adsorption from uranyl acetate solutions. *J. Appl. Polym. Sci.* **88**, 2028 (2003).
51. <http://home.fuse.net/clymer/buffers/phos2.html>.
52. P.J. Flory: *Principles of Polymer Chemistry* (Cornell University, Ithaca, 1953).
53. M. Susoff and W. Oppermann: Influence of cross-linking on probe dynamics in semidilute polystyrene systems. *Macromolecules* **43**, 9100 (2010).